Inorganica Chimica Acta, 111 (1986) 171–178

The Structures of Solvated Methylmercury(II) Chloride, Bromide and Iodide in Pyridine Solution; Implications for Aqueous Solution

A. IVERFELDT*

Department of Inorganic Chemistry, Chalmers University of Technology and University of Göteborg, S-41296 Gothenburg, Sweden

and I. PERSSON

Inorganic Chemistry 1, Chemical Center, University of Lund, P.O. Box 124, S-22100 Lund, Sweden

Received June 6, 1985

Abstract

The structures of solvated methylmercury(II) halides in pyridine solution were determined by a large angle X-ray scattering technique. Near-linear CH_3HgX (X = Cl, Br and I) species solvated by two weakly-coordinated pyridine molecules are indirectly interpreted. Additional mercury–pyridine interactions, through van der Waals forces, are found at the sum of the van der Waals radii. The Hg–X bond distances in the methylmercury(II) halides are found to be 2.325(8), 2.480(3) and 2.649(3) Å for chloride, bromide and iodide, respectively. The Hg-C bond distances are assumed to be ~2.08 Å. This interaction is indicated in the radial distribution functions. The bond distance between mercury and the two solvating pyridine molecules is ~2.8 Å, e.g., 2.84(2) Å in methylmercury(II) bromide. The additional mercury interactions with roughly two pyridine molecules at the sum of van der Waals radii are revealed at around 3.15 Å. Comparison between Raman stretching vibrations and the solvated structures of methylmercury(II) complexes found in various solvents indicates a lower limit in solvent donor property for the formation of solvate bonds to mercury for the methylmercury(II) halides.

Introduction

The importance of distribution equilibria of mercury species between air and water, Henry's law constant, H, in assessing transport and accumulation pathways in the environment has previously been discussed [1–3]. Structural, spectroscopic and thermodynamic studies of various mercury species in solution can explain the magnitude of their Henry's law constant, e.g. geometry, heat and entropy of solvation. The effect on the Henry's law constant of solvent interactions with the mercury species is important [3]. Various thermodynamic solvation data for some methylmercury(II) compounds in water and pyridine can be found elsewhere [1, 3].

The structure determination of methylmercury(II) hydroxide in aqueous solution by a large angle X-ray scattering (LAXS) technique was performed in a previous investigation [4]. The shortest mercury–water distance found was in close agreement with the sum of the mercury and oxygen van der Waals radii [5, 6]. Consequently, water is absent from the inner coordination sphere of mercury. This implies a linear or a nearly linear geometry of methylmercury(II) hydroxide in water; in spite of that, a direct angle determination could not be performed. The solvation of methylmercury(II) hydroxide in water is due to van der Waals forces and hydrogen bonding to the hydroxide group. The strong hydrogen bonding in this case indicates a lower Henry's law constant than, for example, for methylmercury(II) chloride. Variation in the entropy of solvation must, however, also be considered.

The methylmercury(II) halides are considered to be the organomercury species of greatest environmental importance after methylmercury(II) hydroxide. The stability constants of all methylmercury(II) halide complexes in aqueous solution are lower than those found for methylmercury(II) hydroxide and increase in the order $Cl^- < Br^- < I^-$ [7]. However, the coordination chemistry of the methylmercury(II) halides in aqueous solution can not be resolved by direct X-ray scattering experiments, due to low olubility of the complexes in water [8].

In the present investigation, scattering experiments were performed on methylmercury(II) halides dissolved in pyridine. Pyridine was selected to demonstrate the ability of a solvent with sufficiently strong donor properties to solvate CH_3HgX complexes in the inner coordination sphere. A slight deviation from the linearity of the methylmercury(II) halides found in the gas phase, as a result of the weak solvent–solute interaction, was expected.

*Author to whom correspondence should be addressed. Present address: Swedish Environmental Research Institute, P.O. Box 5207, S-40224 Gothenburg, Sweden.

0020-1693/86/$3.50

Variations in the Hg–X and Hg–C stretching frequencies in CH_3HgX when dissolved in various solvents are correlated with the electron-donating properties of the solvents, *i.e.*, the ability to solvate CH_3HgX. Deviation from linearity in solvated HgX_2 molecules has been derived by LAXS, Raman and infrared measurements [9]. The ν(Hg–X) symmetric stretching frequencies decrease with increasing solvent interactions [10]. The occurrence of similar, but considerably weaker, mercury–solvate bonds is thus expected in the pyridine-solvated CH_3HgX complexes.

Differences in the solvate structures from the coordination of a methyl group to mercury are revealed by comparison with HgX_2 (X = Cl, Br and I) structures in pyridine [9] and in the gas phase [11–13]. Compared to inorganic mercury(II), solvated methylmercury(II) compounds show a more pronounced preference for a linear configuration, *i.e.*, the predominant linear or near-linear two-coordination of mercury in $CH_3Hg(II)$ [14].

Additional weak interactions may, however, result in the formation of a second complex at high ligand concentrations, e.g., $CH_3HgI_2^-$ in aqueous solution [7]. The absence of similar chloride and bromide complexes may result from the decrease in electron-donating capacity, ($I^- > Br^- > Cl^-$) [7]. The strong donating properties of both sulfur and nitrogen have also been demonstrated. The existence of $CH_3Hg(SCN)_3^{2-}$ was reported from spectroscopic investigations [15]. However, NMR spectroscopic support was presented for an unchanged mercury hybridization between these stepwise complexes. The magnitude of the formation constants of the pyridine and bipyridine complexes in aqueous solution gave strong indication of a coordination number higher than 2 [16]. The corresponding crystal structure of the methylmercury(II) bipyridine complex showed an irregular three-coordination [17]. The indicated mercury hybridization independence of coordination number in methylmercury(II) species was further evidenced by NMR [18].

Experimental

Chemicals

Weighed amounts of commercial CH_3HgCl (Merck), CH_3HgBr (Ventron) and CH_3HgI (Ventron) were dissolved in pyridine p.a. (Fluka). The compositions of the solutions are given in Table I. Methylmercury(II) iodide carefully prepared for spectroscopic measurements has been reported to contain unremovable traces of inorganic mercury(II) [19]. In addition, slight decomposition of methylmercury(II) compounds during illumination [19] and/or a disproportionation to dimethylmercury and inorganic mercury enhanced by pyridine [20] may occur.

TABLE I. Composition of Experimental Solutions (mol l^{-1})

	CH_3HgCl	CH_3HgBr	CH_3HgI
Hg	1.21	1.43	1.20
Cl	1.21		
Br		1.43	
I			1.20
N	8.50	8.50	8.50
C	43.71	43.93	43.70
H	46.13	46.79	46.10
μ[a]	29.34	43.10	34.27
ρ[b]	0.976	1.073	1.083

[a]μ is the linear absorption coefficient in cm^{-1}, for Mo Kα radiation. [b]ρ is the density at 25 °C in g cm^{-3}.

However, the results indicate no detectable influence compared to the strongly predominant CH_3HgX species.

X-ray Scattering Measurements

A large angle θ–θ diffractometer, described previously [21–23], was used in the scattering experiments at 25 ± 1 °C. The methylmercury(II) solutions were enclosed in a cylindrical thin-walled glass container mounted within the sample housing of the diffractometer [4, 9]. The absorption and angle dependence of the glass container have previously been determined and are described elsewhere [4, 9]. Mo Kα (λ = 0.7107 Å) radiation was used as X-ray source. Scattered intensities from the surface of the solution were determined at discrete points in the interval $5° < \theta < 63°$, separated by 0.1° up to $\theta = 30°$ and by 0.25° for $\theta > 30°$. The scattering angle is 2θ. An extrapolation of the intensity data at $\theta < 5°$ was necessary due to the upward meniscus in the glass container [4, 9]. A counting error of 0.35% was achieved by measuring 40 000 counts twice at each sampling point. The fraction of incoherent scattering contributing to intensity determinations was estimated in the usual manner [24].

Data Treatment

The measured intensity data were corrected for background and polarization and normalized to a stoichiometric unit of volume (V) containing one Hg atom. The corrected intensities were scaled with a factor obtained from the high s region, $s > 13.5$ $Å^{-1}$, where the scattering variable $s = 4\pi \sin\theta/\lambda$. The comparison of experimental and independent theoretical scattering in this region was found to be in good agreement with a standard integration procedure [25, 26]. Scattering factors, f for neutral atoms [27], the spherical form factor for H [28], anomalous dispersion ($\Delta f'$ and $\Delta f''$) for the various atoms [27], and corrected [29, 30] incoherent scattering factors [31–

33] were applied to derive the reduced intensities, $i(s)$, from the scaled observed intensities, $I_{obs}(s)$.

$$i(s) = I_{obs}(s) - \sum_m [(f_m(s) + \Delta f'_m)^2 + (\Delta f''_m)^2]$$

The fraction of incoherent radiation reaching the counter, $del(s)$, was also considered in the incoherent correction [24].

A Fourier transformation was applied to obtain the differential radial distribution function, RDF = $D(r) - 4\pi r^2\rho_0$

$$D(r) - 4\pi r^2\rho_0 = (2r/\pi)\int_0^{s_{max}} si(s)M(s)\sin(rs)ds$$

where the average scattering density, ρ_0, is given by

$$\rho_0 = \left\{\left[\sum_m (f_m + \Delta f'_m)\right]^2 + \left(\sum_m \Delta f''_m\right)^2\right\} \Big/ V$$

The effect of the modification function, $M(s)$, where

$$M(s) = [f_{Hg}^2(0)/f_{Hg}^2(s)]\exp(-0.01s^2)$$

is described in detail elsewhere [9].

Calculations of reduced intensities, $i_{calc}(s)$, from interatomic interactions in the plausible models were performed as described previously [34]. The $i_{calc}(s)$ was treated in the same manner as the experimental reduced intensities in order to derive completely comparable radial distribution functions. Spurious peaks below 1.5 Å were removed from the RDF by a procedure described elsewhere [21].

The calculations were performed by means of the KURVLR program [34], while least-squares refinements of the significantly resolvable interactions in the models were carried out using the PUTSLR [34] and STEPLR [35] programs. The differences between the observed and calculated reduced intensities were minimized in the refinements according to

$$U = \sum_{s_{min}}^{s_{max}} w(s)[i_{obs}(s) - i_{calc}(s)]^2$$

with the weighting function, $w(s)$, proportional to $I_{obs}^{-2}\cos\theta$ for each point.

Results and Discussion

The predominant distances within the methylmercury(II) halide pyridine solutions may be derived directly from the differential radial distribution function, RDF (see Figs. 1a, 2a and 3a).

Pyridine itself gives rise to the peak at 1.4 Å through the N–C and C–C bond distances. The intramolecular non-bonding distances in pyridine at 2.4 and 2.7 Å are more difficult to detect since they overlap with the predominant Hg–X interactions.

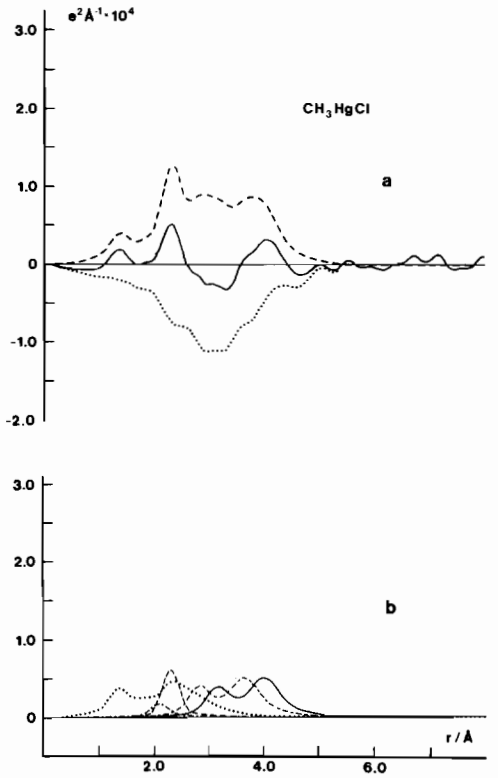

Fig. 1. (a) Experimental differential radial distribution function, $D(r) - 4\pi r^2\rho_0$, for the methylmercury(II) chloride in pyridine solution (——), the sum of theoretical interaction (– – –), and the calculated difference between the theoretical and experimental RDF (· · ·). (b) Calculated specific interactions and their contribution to the RDF model function: pyridine structure (· · ·), the Hg–CH_3 interaction (– · –), the Hg–Cl interaction (- - -), the closest Hg–pyridine interaction (– – –), the Hg–pyridine interaction, where pyridine is found around the sum of van der Waals radii (——).

The peaks arising from pyridine were interpreted from the crystal structures of $HgCl_2(py)_2$ and $HgBr_2(py)_2$ [36]. The magnitude and location of the contributions from the solvent in the RDF are shown by the theoretical peak shapes in Figs. 1b, 2b and 3b.

The calculated peak shapes of the main interactions in the methylmercury(II) halides (Hg–X and Hg–C distances) display various degrees of overlap (see Figs. 1b, 2b and 3b). The predominant peaks at 2.3, 2.5 and 2.6 Å for the methylmercury(II) chloride, bromide and iodide solutions, respectively, result mainly from the Hg–X bond distances. The Hg–C bond distance in the solvated methylmercury(II) halides, expected to occur at about 2.1 Å (see Table II), is observed only as an asymmetry in the Hg–I peak. The Hg–C distance in methylmercury(II) chloride and bromide is hidden by the intramolecular pyridine and the Hg–X interactions.

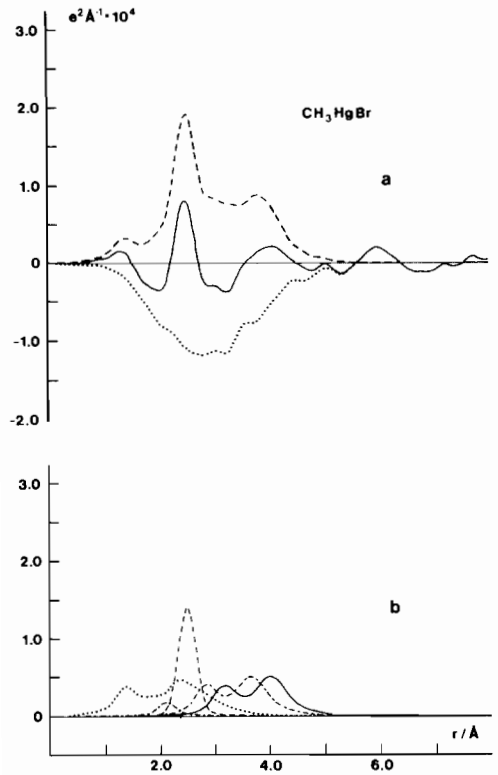

Fig. 2. (a) Experimental differential radial distribution function, $D(r) - 4\pi r^2\rho_0$, for the methylmercury(II) bromide in pyridine solution (——), the sum of theoretical interaction (– – –), and the calculated difference between the theoretical and experimental RDF (· · ·). (b) Calculated specific interactions and their contribution to the RDF model function: pyridine structure (· · ·), the Hg–CH_3 interaction (– · –), the Hg–Br interaction (- - -), the closest Hg–pyridine interaction (– – –), the Hg–pyridine interaction, where pyridine is found around the sum of van der Waals radii (——).

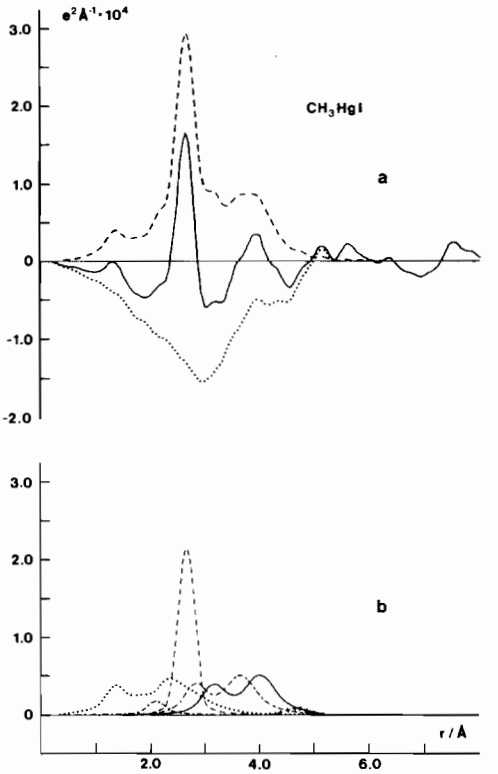

Fig. 3. (a) Experimental differential radial distribution function, $D(r) - 4\pi r^2\rho_0$, for the methylmercury(II) iodide in pyridine solution (——), the sum of theoretical interaction (– – –), and the calculated difference between the theoretical and experimental RDF (· · ·). (b) Calculated specific interactions and their contribution to the RDF model function: pyridine structure (· · ·), the Hg–CH_3 interaction (– · –), the Hg–I interaction (- - -), the CH_3–I interaction (+ + +), the closest Hg–pyridine interaction (– – –), the Hg–pyridine interaction, where pyridine is found around the sum of van der Waals radii (——).

TABLE II. Bond Distances Found within CH_3HgX (X = Cl, Br and I) in Gas Phase[a] and in Pyridine Solution Compared to Distances in HgX_2 Complexes (Å)

Complex	Gas		Pyridine
	Hg–X	Hg–C	Hg–X
CH_3HgCl	2.283[b]	2.055[b]	2.325(8)[c]
$HgCl_2$	2.27[d]		2.375[e]
CH_3HgBr	2.406[b]	2.072[b]	2.480(3)[c]
$HgBr_2$	2.41[f]		2.497[e]
CH_3HgI	2.571[b]	2.077[b]	2.649(3)[c]
HgI_2	2.59[f]		2.665[e]
CH_3HgCH_3		2.080[g]	

[a]Determined by microwave measurements. [b]Ref. 42. [c]Present study. [d]Ref. 13. [e]Ref. 9. [f]Refs. 11 and 13. [g]Derived from electron diffraction measurements [43].

Comparisons between the a and b parts of Figs. 1, 2 and 3 clearly demonstrate the accuracy and relative importance of the calculated specific interactions. Also revealed is the possibility of distinguishing between various separte interactions. The calculated contributions from the C–X interaction in the methylmercury(II) halides are even less than the minor contribution from Hg–C and are, further, found in a more complex region of the RDF. This shows why a direct determination of the C–Hg–X angle is impossible for all three solutions. In this case, deviation from linearity can not be proved by this technique and thus can not be used as a measure of degree of solvation. An indication of a shoulder at 4.7 Å in the experimental RDF (the expected C–I distance in a linear configuration) can possibly be assigned to this distance.

The interpretation of Hg–N distances in solvated methylmercury(II) halides is important in resolving the solvation strength. The Hg–N bond distance is shown only as a slight asymmetry on the Hg–X peak in the RDF values of CH_3HgBr and CH_3HgI, because of the dominating Hg–X interaction, Figs.

2 and 3. This distance has less overlapping in CH_3HgCl and, further, the contribution from Hg–N to the RDF is relatively strong. A significant shoulder at about 2.8 Å is also found in the experimental curve and is assigned to be the Hg–N bond distance of the pyridine-solvated methylmercury(II) chloride. The Hg–N bond distance is rather long but still considerably shorter than the sum of van der Waals radii. This is a clear indication of a mercury–solvent interaction, although rather weak. Small peaks are found at the sum of van der Waals radii, around 3.2 Å, for all three methylmercury(II) halide solutions. Steric hindrance is certainly not present and additional pyridine may appraoch CH_3HgX. These interactions are due to the van der Waals force solvation of the methylmercury(II) halides. As described elsewhere [4], the maximum van der Waals radius given in literature for Hg, 1.73 Å [5, 6], is applied. A minimum van der Waals radius of 1.42 Å for nitrogen (pyridine) is consequently found. The van der Waals radius given in literature for nitrogen is 1.50 Å [37].

The Hg–N distances in the structures of the solvated methylmercury(II) halides were supported as previously reported [9] for inorganic mercury(II) halides in pyridine. Geometrical calculations based on parameters from the pyridine ring in the solid state structure of $HgBr_2(py)_2$ [36] predict peaks in the RDF for the shortest mercury-pyridine interaction arising from Hg–C(2,6), Hg–C(3,5) and Hg–C(4) at 3.7, 5.0 and 5.6 Å, respectively. The longer mercury–pyridine interaction implies peaks 0.3 Å further out. Some of these Hg–C distances are also shown in Figs. 1a, 2a and 3a. The diffuse Hg–N bond distance in the RDF arising from the solvated methylmercury(II) bromide could also be revealed from the least-squares refinements.

In an effort to use the experimental data and data from the literature in an appropriate way, only supported bond distances were taken into the models. The mercury–halide and mercury–carbon distances within methylmercury(II) halides were used in the proposed structural model, together with two different distances between mercury and the solvating pyridine molecules, Hg–N and Hg–C(2,6). The number of pyridine molecules, two at both distances, were derived from peak sizes. The remaining peaks in the RDF above 4 Å refer to intermolecular distances which have not been refined.

Least-squares refinements of significant parameters within the models were performed. The results are summarized in Table III. The refined parameters were restricted to Hg–X and Hg–N interactions. Various lower s limits were used (between 3.5 and 5.0). The fixed parameters in models were varied and simpler models applied to ensure that no effects on refined interactions occurred through overlapping distances or poor models.

TABLE III. Interaction within the Model Describing Solvation of CH_3HgX (X = Cl, Br and I) in Pyridine[a]

Interaction		CH_3HgCl[b]	CH_3HgBr[c]	CH_3HgI[d]
Hg–X	*d*	2.325(8)	2.480(3)	2.649(3)
	b	0.002	0.0030(4)	0.002
	n	1.0	1.0	1.0
Hg–C	*d*	2.07	2.08	2.09
	b	0.002	0.002	0.002
	n	1.0	1.0	1.0
Hg–N	*d*	2.84	2.84(2)	2.84
	b	0.008	0.006(2)	0.008
	n	2.0	2.0	2.0
Hg–C(2,6)	*d*	3.65	3.65	3.65
	b	0.020	0.020	0.020
	n	4.0	4.0	4.0
Hg–N[e]	*d*	3.15	3.15	3.15
	b	0.008	0.008	0.008
	n	2.0	2.0	2.0
Hg–C(2,6)[e]	*d*	4.00	4.00	4.00
	b	0.018	0.018	0.018
	n	4.0	4.0	4.0

[a]Refined parameters from experimental data given with standard deviations in parentheses; distance: *d*, Å; temperature coefficient: *b*, Å^2; *n*: number distances/mercury atom. [b]The least-squares refinements were performed in the range $5.0 \leq s \leq 15.5$ Å^{-1}. [c]Refinements in the range $3.5 \leq s \leq 15.5$ Å^{-1}. [d]Refinements in the range $4.5 \leq s \leq 15.5$ Å^{-1}. [e]Pyridine at the sum of van der Waals radii.

The complete models for the solvated methylmercury(II) halides are given in Table III and shown in Figs. 1, 2 and 3. The three smooth difference curves are comparable and have the same shape as the curves for HgX_2 in pyridine [9]. The small ripples left in the range 3.5 Å to about 5.5 Å most certainly arise from intermolecular distances between the methylmercury(II) complex and the pyridine molecules. It is impossible to include these interactions in an adequate model, because of the large number of distances and the lack of supporting structural data from the solid phase. The fit of the calculated reduced intensity data with the experimental data is satisfactory from below 4 Å^{-1} (Fig. 4). Long range interactions, not included in the models, are prominent only at very low s values.

A comparison with crystal structures of nitrogen-donating aromatic uni-, bi- and tri-dentates reveals Hg–N distances and C–Hg–N angles and their dependence on coordination number of mercury [17, 38–41]. Besides the shortest Hg–N distance involved in the C–Hg–N moiety, additional coordinated nitrogen is found in the interval 2.43–2.75 Å. The polydentates are considered to represent a lower limit of the C–Hg–N angles and the additional bond distances. The upper limit is derived from the linear methylmercury(II) complexes with pyridine [38]

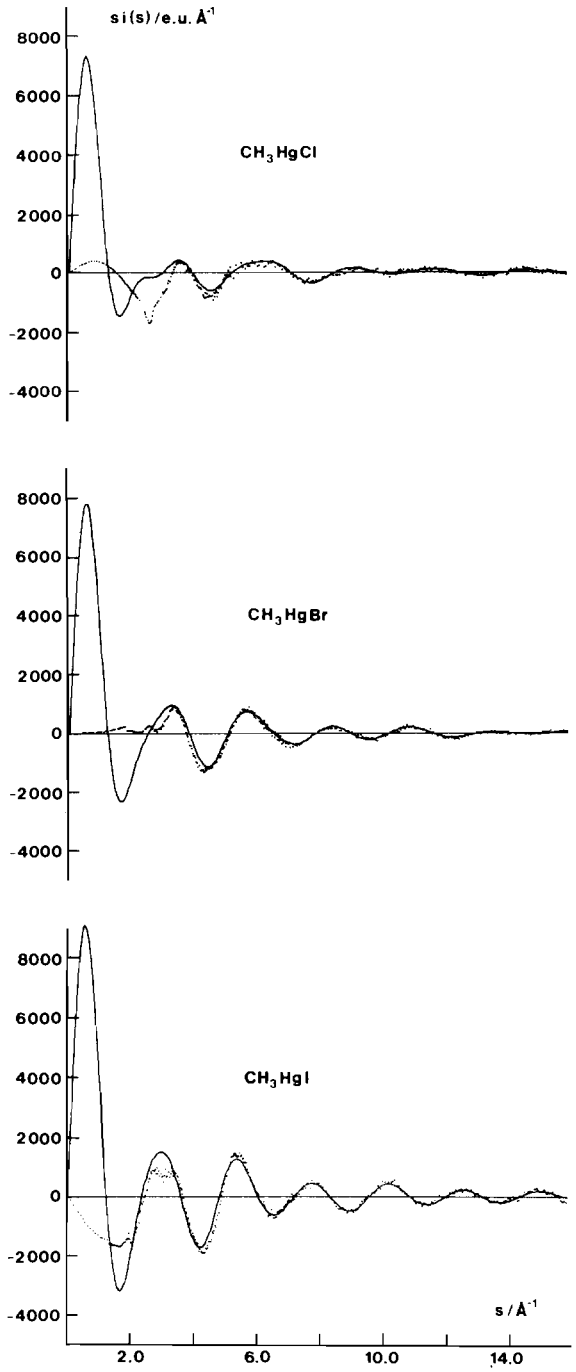

Fig. 4. Experimental *si(s)* values (dots) and values calculated from models of the solvated methylmercury(II) halides (——). The parameters used in the respective models are given in Table III.

and 2-benzylpyridine [40], where no additional Hg–N interactions are present.

The Hg–C distances in the solid methylmercury(II) complexes, 2.01–2.10 Å, are comparable with the bond distances in gaseous phase [42, 43] and in the present pyridine solutions. The negligible effect of change in coordination number on the Hg–C distance is consistent with the remaining sp hybridization [18, 39], and supports the theory that there is a significant difference in the solvating Hg–N bond lengths between methylmercury(II) and inorganic mercury(II) halides.

A strong correlation between increasing donor properties of the solvent, decreasing stretching frequencies ν(Hg–X), decreasing X–Hg–X angles and increasing Hg–X bond distances has been found in the solvated HgX_2 (X = Cl, Br and I) complexes [9, 10]. The Raman stretching frequencies reported for the methylmercury(II) halides in various solvents are listed in Table IV. A stronger mercury-solvent interaction of the methylmercury(II) halides in pyridine compared to aqueous solution is supported by the decrease in the ν(Hg–X) frequency.

A striking result derived from Table IV is that solvent–mercury interactions seem to occur above a lower limit in the electron-donating properties of the solvent. Among the solvents studied, only the strong-donating pyridine appears to exhibit any coordinating tendency to mercury in methylmercury(II). The lower limit of the solvation properties of a solvent to form a solvate bond to inorganic mercury(II) halides is much less, and the decrease in ν(Hg–X) frequencies is also more pronounced [9]. This is in agreement with stronger solvate bonds to HgX_2 than to CH_3HgX species for the same solvent. The enlargement of Hg–N distance in solvated methylmercury(II) halides is therefore expected. The Hg–N bond lengths for the pseudo-tetrahedral $HgX_2(py)_2$ in pyridine vary from 2.43 to 2.51 Å [9]. No Hg–N distance corresponding to the sum of van der Waals radii can be found in these solutions. The longer Hg–N bond distance, at about 2.8 Å, and the larger X–Hg–X angle in the structures of the solvated methylmercury(II) halides give space for additional pyridines at the sum of van der Waals radii.

The linearity of methylmercury(II) hydroxide in aqueous solution is strongly evidenced by the fact that no water can be found at a distance from mercury shorter than the sum of van der Waals radii [4]. The hydrogen bonds to the hydroxide group will have no influence on the linearity. The Raman data of methylmercury(II) halides dissolved in various solvents, summarized in Table IV, show that pyridine solvates significantly better than the other solvents. Benzene, carbon tetrachloride, methanol and water obviously do not have sufficiently strong solvation properties to form solvate bonds to mercury in methylmercury(II) complexes. Neutral methylmercury(II) complexes without mercury–solvate bonds are certainly also linear in solution. The Hg–X bond distances in solution compared with

TABLE IV. Raman Stretching Vibration (cm^{-1}) for Methylmercury(II) Species in Different Solvents Compared to Inorganic Mercury(II) Halides. Gaseous and Solid Phase Data are Included as References

Complex	Gas	Solid	Solvent				
			Benzene	CCl_4	Methanol	Water	Pyridine
CH_3HgF							
ν(Hg–Cl)						573[a]	
ν(Hg–F)						414[a]	
CH_3HgOH							
ν(Hg–C)						570[b]	
ν(Hg–O)						504[b]	
CH_3HgCl							
ν(Hg–C)		554[c]	554[c]		554[e]	556[d]	547[e]
ν(Hg–Cl)		293 288[c]	336[c]		328[e]	334[d]	316[e]
CH_3HgBr							
ν(Hg–C)		546[c]	545[c]		546[e]	546[d]	535[e]
ν(Hg–Br)		204[c]	228[c]		225[e]	228[d]	212[e]
CH_3HgI							
ν(Hg–C)		530[c]	533[c]		535[e]	535[d]	528[e]
ν(Hg–I)		166[c]	181[c]		178[e]	181[d]	175[e]
CH_3HgCH_3							
ν(Hg–C)		514[f]		514[g]			
$HgCl_2$							
ν(Hg–Cl)	358[h]		339[i]		324[i]	320[i]	283[j]
$HgBr_2$							
ν(Hg–Br)	222[h]		213[i]		206[i]	205[i]	183[j]
HgI_2							
ν(Hg–I)	158[h]				151[i]		142[j]

[a]Ref. 48. [b]Ref. 4. [c]Ref. 19. [d]Ref. 47. [e]Ref. 44. [f]In liquid state [45]. [g]Ref. 46. [h]Ref. 50. [i]Ref. 49. [j]Ref. 10.

gaseous phase will depend on the solvation of the ligand. In aqueous solution the hydration decreases in the order $OH^- > Cl^- > Br^- > I^-$. The Hg–C bond distances are probably fairly unaffected by the solvent; this is also supported by the Raman data.

Conclusions

The solvated structure of methylmercury(II) halides in pyridine was interpreted from X-ray scattering studies. It is suggested that the Hg–C bond distances in CH_3HgX remain almost the same as in the gaseous phase. This is consistent with the prevailing mercury sp hybridization for Hg coordination numbers larger than 2. The Hg–X distances are significantly shorter than the Hg–X distances in pyridine solutions of HgX_2. The Hg–N bond distance of the two solvating pyridine molecules is 0.4 Å longer and the C–Hg–X angle is larger than found in the mercury(II) halides. This results in more space for additional pyridine to interact via van der Waals forces. The presence of pyridine molecules at the sum of van der Waals radii is confirmed. Raman data from literature also show that methylmercury(II) halides are less solvated than HgX_2 in pyridine.

Comparison of Raman stretching vibrations in various solvents and the solvated structure of methylmercury(II) hydroxide in water indicated that CH_3-HgX species were solvated by van der Waals forces only in solvents with weaker donor properties than pyridine. This conclusion will have great importance for the interpretation of the solvated structures of methylmercury(II) halides in water. It is thus suggested that the methylmercury(II) halides have a linear structure and have water only at the sum of van der Waals radii for Hg and O. The Hg–X bonds in water are probably slightly extended compared with the gaseous phase depending on van der Waals forces and hydration of the halide through hydrogen bonds. The absence of stronger interactions with water provides an explanation, on a structural basis, of why the tendency to distribute to gas phase (a larger Henry's law constant, H) is more pronounced for the methylmercury(II) halides compared to HgX_2. Generally, the difference in solvation between the ligands (e.g., the hydroxide, halides and methyl groups) and the variation in solvation entropy must also be considered.

References

1 Å. Iverfeldt and O. Lindqvist, *Atmos. Environ., 16*, 2917 (1982).
2 O. Lindqvist and H. Rodhe, *Tellus*, (1985) in press.
3 Å. Iverfeldt and I. Persson, *Inorg. Chim. Acta, 103*, 113 (1985).
4 Å. Iverfeldt and I. Persson, *Inorg. Chim. Acta, 111*, 179 (1986).
5 D. Grdenic, *Q. Rev., 19*, 303 (1965).
6 A. J. Canty and G. B. Deacon, *Inorg. Chim. Acta, 45*, L225 (1980).
7 G. Schwarzenbach and M. Schellenberg, *Helv. Chim. Acta, 48*, 28 (1965).
8 T. Waugh, H. F. Walton and J. A. Laswick, *J. Phys. Chem., 59*, 395 (1955).
9 I. Persson, M. Sandström, P. L. Goggin and A. Mosset, *J. Chem. Soc., Dalton Trans.*, 1597 (1985).
10 I. Persson, M. Sandström and P. L. Goggin, to be submitted for publication.
11 K. Kasiwabara, S. Konaka and M. Kimura, *Bull. Chem. Soc. Jpn., 46*, 410 (1973).
12 L. R. Maxwell and V. M. Mosley, *Phys. Rev., 57*, 21 (1940).
13 P. A. Akishin, V. P. Spiridonov and A. N. Khodchenkov, *Zh. Fiz. Chim., 33*, 20 (1959).
14 D. L. Rabenstein, *Acc. Chem. Res., 11*, 100 (1978).
15 J. Relf, R. P. Cooney and H. F. Henneike, *J. Organomet. Chem., 39*, 75 (1972).
16 G. Anderegg, *Helv. Chim. Acta, 57*, 1340 (1974).
17 A. J. Canty and B. M. Gatehouse, *J. Chem. Soc., Dalton Trans.*, 2018 (1976).
18 A. J. Canty and A. Marker, *Inorg. Chem., 15*, 425 (1976).
19 P. L. Goggin, G. Kemeny and J. Mink, *J. Chem. Soc., Faraday Trans. 2, 72*, 1025 (1976).
20 L. L. Murell and T. L. Brown, *J. Organomet. Chem., 13*, 301 (1968).
21 H. A. Levy, M. D. Danford and A. H. Narten, 'Data Collection and Evaluation with an X-Ray Diffractometer Designed for the Study of Liquid Structure', Report ORNL-3960, Oak Ridge National Laboratory, Oak Ridge, Tenn., 1966.
22 G. Johansson, *Acta Chem. Scand., 20*, 553 (1966).
23 M. Sandström and G. Johansson, *Acta Chem. Scand., Ser. A:, 31*, 132 (1977).
24 M. Sandström, I. Persson and S. Ahrland, *Acta Chem. Scand., Ser. A:, 32*, 607 (1978).
25 J. Krogh-Moe, *Acta Crystallogr., 9*, 951 (1956).
26 N. Norman, *Acta Crystallogr., 10*, 370 (1957).
27 'International Tables for X-Ray Crystallography, Vol. 4', Kynoch Press, Birmingham, 1974.
28 R. F. Stewart, E. R. Davidson and W. T. Simpson, *J. Chem. Phys., 42*, 3175 (1965).
29 G. Breit, *Phys. Rev., 27*, 362 (1926).
30 P. A. M. Dirac, *Proc. R. Soc. London, Ser. A:, 111*, 405 (1926).
31 D. T. Cromer and J. B. Mann, *J. Chem. Phys., 47*, 1892 (1967).
32 D. T. Cromer, *J. Chem. Phys., 50*, 4857 (1969).
33 A. H. Compton and S. K. Allison, 'X-Rays in Theory and Experiment', Van Nostrand-Reinhold, New York, 1935.
34 G. Johansson and M. Sandström, *Chem. Scr., 4*, 195 (1973).
35 M. Molund and I. Persson, *Chem. Scr., 25*, 197 (1985).
36 A. J. Canty, C. L. Raston, B. W. Skelton and A. W. White, *J. Chem. Soc., Dalton Trans.*, 15 (1982).
37 L. Pauling, 'The Nature of the Chemical Bond', Cornell University Press, Ithaca, 1960.
38 R. T. C. Brownlee, A. J. Canty and M. F. Mackay, *Aust. J. Chem., 31*, 1933 (1978).
39 A. J. Canty, N. Chaichit, B. M. Gatehouse, E. E. George and G. Hayhurst, *Inorg. Chem., 20*, 2414 (1981).
40 A. J. Canty, N. Chaichit and B. M. Gatehouse, *Acta Crystallogr., Sect. B:, 36*, 786 (1980).
41 A. J. Canty, N. Chaichit, B. M. Gatehouse and A. Marker, *Acta Crystallogr., Sect. B:, 34*, 3229 (1978).
42 C. Walls, D. G. Lister and J. Sheridan, *J. Chem. Soc., Faraday Trans. 2*, 1091 (1975).
43 K. Kashiwabara, S. Konaka, T. Iijima and M. Kimura, *Bull. Chem. Soc. Jpn., 46*, 407 (1973).
44 K. Sone, M. Aritaki, K. Hiraoka and Y. Fukuda, *Bull. Chem. Soc. Jpn., 49*, 2015 (1976).
45 P. L. Goggin and L. A. Woodward, *Trans. Faraday Soc., 56*, 1591 (1960).
46 P. L. Goggin and N. W. Hurst, *J. Chem. Res. (M)*, 4713 (1978).
47 P. L. Goggin and L. A. Woodward, *Trans. Faraday Soc., 62*, 1423 (1966).
48 D. Breitinger, A. Zober and M. Neubauer, *J. Organomet. Chem., 30*, C49 (1971).
49 J. H. Smith and T. B. Brill, *Inorg. Chim. Acta, 18*, 225 (1976).
50 R. H. J. Clark and D. M. Rippon, *J. Chem. Soc., Faraday Trans., 2*, 1496 (1973).